Macromolecules

Article

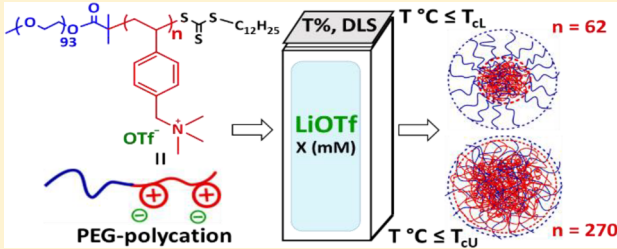# Molecular Mass Affects the Phase Separation of Aqueous PEG–Polycation Block Copolymer

Vikram Baddam, Reetta Missonen, Sami Hietala, and Heikki Tenhu*

Department of Chemistry, University of Helsinki, PB 55, FIN-00014 Helsinki, Finland

S *Supporting Information*

ABSTRACT: Mechanisms of the phase separation and remixing of cationic PEG-containing block copolymers have been investigated in aqueous lithium triflate solutions. The polycation was poly(vinylbenzyl trimethylammonium triflate). We have previously reported on one such block copolymer, which upon cooling of a hot clear solution first underwent phase separation into a turbid colloid and, later, partially cleared again with further cooling. To better understand the balance of various interactions in the solutions/dispersions, a series of polymers with varying DP of the cationic block was synthesized. From one of the

polymers, the alkyl end group (a fragment of the chain transfer agent) was removed. The length of the cationic block affected critically the behavior, but the hydrophobic end group had a minimal effect. Polymers with a short cationic block turn cloudy and partially clear again during a temperature decrease, whereas those with a long cationic block phase separate and slowly precipitate and remix only when heated. Phase separation takes place via particle formation, and we suggest different mechanisms for colloidal stabilization of particles composed of short or long chains.

INTRODUCTION

Polycations can be changed from water-soluble to insoluble by introducing hydrophobic counterions, as tetrafluoroborate (BF_4^-), hexafluorophosphate (PF_6^-), trifluoromethanesulfonate ($CF_3SO_3^-$ or OTf), and bis(trifluoromethane)sulfonimide ($[(CF_3SO_2)_2N]^-$ or NTf_2) anions.[1−3] In addition, the counterions can turn the polymers thermosensitive with either UCST or LCST owing not only to their hydrophobicity but also to ionic interactions between the cationic repeating units and the ions.[4−9] In case of aqueous cationic homopolymers, the stability of phase-separated colloids depends on the concentration of the hydrophobic anions. With high concentration, the polycations precipitate. On the other hand, increasing the concentration of a simple salt as NaCl may lead to the dissolution of the polymer.[5]

As is the case with aqueous nonionic polymers, the phase separation temperature of polycations can be regulated by hydrophobic or hydrophilic structural units added as comonomers, side chains or end groups. The phase separation of copolymers consisting of nonionic and cationic repeating units has been intensely explored, good examples being poly(N-isopropylacrylamide) (PNIPAM) copolymers,[10−13] poly(2-hydroxyethyl methacrylate) (PHEMA),[14] poly(oligo-(ethylene glycol) methacrylate) (POEGMA),[15] poly(ethylene glycol) (PEG),[16,17] and poly[oligo(2-ethyl-2-oxazoline)-acrylate] P(OEtOxA).[18] Other cationically derivatized polymers include poly(propylene glycol) (PPG),[19] poly(γ-propyl-L-glutamate) (PPLG),[20] poly(γ-2-ethoxyethyl-L-glutamate) (PEELG),[21] and poly(γ-3-azidopropyl-L-glutamate) (PAPLG).[22] The changes in the phase separation processes

induced by the cationic units may be profound and the system may even change from a LCST to an UCST one.

We recently reported[17] studies on the phase behavior of a block copolymer poly(ethylene glycol)-b-poly-(vinylbenzyltrimethylammonium triflate), PEG₉₃-PVBTMA₈₁-OTf. The idea of choosing this polymer was to see if we can stabilize phase-separated polycation colloids with the PEG blocks. The system turned out, however, to be more complicated than anticipated. The aqueous block copolymer undergoes a stepwise phase separation in aqueous trifle solutions during cooling. When a hot, clear solution is cooled, it suddenly turns turbid but with further cooling starts to clear. On the other hand, the cationic homopolymer shows only UCST. A phase separation mechanism for the PEG₉₃-PVBTMA₈₁-OTf was proposed where the interactions between the counterions, cationic repeating units, and PEG blocks govern the dissolution and aggregation of the polymers. In this case, the PEG and polycation blocks had DPs very close to each other (93 and 81, correspondingly), and a possibility remains that the equal numbers of interacting units prevent the total phase separation of the polymer. To better understand the phase separation processes, we needed to extend the investigation and find out, what is the effect of the length ratio of the two blocks. Because of the RAFT agent used in the syntheses, the polymers carried a dodecyl end group, so we also wanted to learn what is the effect of those hydrophobes.

Table 1. List of Block Copolymers Synthesized by RAFT

polymer	[M]:[CTA]:[I]	conversion of VBTMA-OTf (%)	DP theor	DP NMR	$M_{n\ Theo}$[a] (g/mol)	$M_{n\ NMR}$[b] (g/mol)	ratio$_{NMR}$[b] [PEG]:[PVBTMA]
VB-62	100:1:0.2	75	75	62	30000	25000	1:0.67
VB-81[c]	100:1:0.2	97	97	81	36500	30700	1:0.9
VB-172	200:1:0.2	97	193	172	67700	60900	1:1.9
VB-270	400:1:0.2	93	372	270	125900	92700	1:2.9

[a]Theoretical molecular mass from the equation [M]/[CTA] × convn × MM + MCTA. M_n of the PEG macro-CTA 5000 g/mol (from Sigma), M_n from SEC is 4900 g/mol with PDI 1.01, and the average DP from ^{1}H NMR is 93. [b]The molar mass and block ratios were determined by ^{1}H NMR. [c]From ref 17.

Therefore, block copolymers comprising a polyethylene glycol block and a polycation, poly(vinylbenzyl trimethylammonium triflate), PVBTMA-OTf, with different molecular weights have been studied. The length of the PEG block was kept constant, and we first wanted to see the effect of increasing length of the polycation on the phase separation behavior. Second, by increasing the number of cationic charges, we expected to get an insight into the interactions involved in the phase-separated colloidal systems. The research questions are of importance, knowing how much PEG is used in solubilizing or hydrophilization of various hydrophobic substances.

In this work, we report the phase separation and remixing of block copolymers PEG-PVBTMA-OTf in aqueous solutions of lithium triflate. We assume the molar mass affects the temperature window between the clouding and clearing of the of the polymer solution. The assumption is based on the above-mentioned facts that, first, we have observed such a window for one block copolymer and, second, homopolymers with no PEG do not experience remixing with lowering temperature.

A reasonably good understanding of the thermal processes can be reached by turbidometric and light scattering techniques. However, we have deepened the investigation by NMR spectroscopy, trying with different techniques to elucidate the molecular level interactions in the PEG$_{93}$-PVBTMA$_n$-OTf. We are able to rationalize the mechanism of the coexistence of the T_{cU} and T_{cL} by terms of the temperature dependent interaction between the triflate anion and the polymer as well as the temperature dependent interactions between the chemically different blocks. Within the insolubility window (or below T_{cU}) all interactions are at their strongest. A general picture emerges where the polymers form colloidal particles immediately when a hot transparent solution is allowed to cool. Temperature-dependent turbidity indicates that the sizes and aggregation states of the particles vary. We assume this is due to different mechanisms of colloidal stability, either steric stabilization with PEG or electrostatic stabilization by the ionic charges.

■ EXPERIMENTAL PART

Materials. PEG macro chain transfer agent, poly(ethylene glycol) methyl ether 2-(dodecylthiocarbonothioylthio)-2-methylpropionate (average M_n 5000 g mol^{-1}) from Sigma-Aldrich was used as received. Preparation of (vinylbenzyl)trimethylammonium triflate [(VBTMA-OTf] and the copolymer VB-81 have been reported previously.[17] 4,4'-Azobis(4-cyanovaleric acid) (ACPA; ≥ 75%, Sigma) and azobis-(isobutyronitrile) (AIBN 98%, from Fluka) were recrystallized from methanol. Trifluoromethanesulfonic acid lithium salt (LiOTf; 99.995%, Sigma), sodium chloride (NaCl; 99.98%), and sodium formate (HCOONA; ≥99.0%) were used as received. Deionized water was purified with an ELGA purelab ultrapurification system.

Distilled water was used in the dialysis. Regenerated cellulose tubings (Orange Scientific) with a molecular weight cutoff of 14000 g mol^{-1} were used in the dialysis. Deuterated DMSO and D$_2$O from Eurisotop were used as NMR solvents.

Syntheses. The block copolymers were synthesized via RAFT polymerization using the same conditions as previously reported.[17] The reagent ratios [monomer]:[CTA]:[ACPA] were varied to obtain different molecular mass polymers. The end group of VB-61 was removed by reacting with AIBN under inert atmosphere at 75 °C. The ratio of [CTA]:[AIBN] used in the reaction was 1:5 (see the Supporting Information). The polymers were purified by dialysis for 2−3 days with changing the distilled water/methanol several times.

Sample Preparation. The stock solutions with concentrations of 10−25 mg mL^{-1} were prepared 1 day prior to the sample preparation. In each sample preparation, salt solutions were first prepared in the vials, and then the corresponding amounts of polymer stock solutions were added with stirring.

^{1}H NMR Spectroscopy. The molar mass (M_n) and the block ratios of the polymers were determined by using Bruker Avance III 500 MHz spectrometer with 256 scans, taking the PEG signal as a reference. The samples with polymer concentration 10 mg mL^{-1} were prepared in DMSO-d_6 for molar mass measurements. Samples consisting of 2 mg mL^{-1} of polymer with 50 mM (150 mM in VB-62) LiOTf and 0.5 mM of HCOONa in D$_2$O were used for the temperature variant ^{1}H NMR and NOESY measurements. All the measurements were conducted by first cooling with 1 °C step from elevated temperature to temperature below the ambient and then heating again. The samples were stabilized 5 min at each temperature. The 2D nuclear Overhauser effect spectroscopy (NOESY) experiments were conducted for polymers at several temperatures upon cooling. The mixing time was 256 ms with 16 scans.

Transmittance. The transmittance curves were collected at 600 nm wavelength as function of temperature. UV−vis spectrophotometer, JASCO V-750 equipped with a JASCO CTU-100 water jacketed Peltier thermostat system was used for all measurements. The temperatures were measured directly from the sample cell. Cooling and heating rates were 1 °C min^{-1} unless otherwise mentioned. The accuracy of T_cs is within ±1 °C.

Before the measurements, the degassed samples were stabilized for 10 min at elevated temperatures (from 70 to 90 °C). The cloud point or clearing temperatures were measured first with stepwise cooling the holder to around 10 °C. The heating cycle was measured after 10 min of stabilization at 10 °C. The temperature ranges were altered in some cases.

Dynamic Light Scattering (DLS). The size distributions and scattered intensities of the polymer solutions were measured at 173° angle as a function of temperature. All data were collected with Malvern Instruments ZetaSizer Nano-ZS equipped with a 4 mW He−Ne laser operating at 633 nm. Prior to the measurement, the samples were stabilized for 10 min at elevated temperature. The hydrodynamic diameters and scattered light intensities were collected while stepwise (5 °C) cooling the solution down to 20 °C, then again with heating. The samples were equilibrated for 5 min at each temperature. Samples consisting of 2 mg mL^{-1} polymer and 50 mM LiOTf, 150 mM in the case of VB-62, were used. The hot solutions were filtered into cuvettes with 0.45 μm Millipore PVDF filters.

Electrophoretic Mobility. Electophoretic mobilities of three polymers were measured using Malvern ZetaSizer Nano-ZS, with voltage 30 V. Here, 50 mM aqueous LiOTf was the solvent, and the polymer concentration was 1 mg/mL. The samples were measured first at 65 °C and, then, after 10 min stabilization at 25 °C. The values reported here are averages of three measurements each.

■ **RESULTS AND DISCUSSION**

Polymerization of VBTMA-OTf via RAFT with PEG macro-CTA. The polymerizations were conducted at 75 °C in water−methanol mixture (Scheme S1). Reaction conditions and the product polymers are listed in Table 1. For simplicity, we from now on refer to the polymers as VB-*n* where *n* is the degree of polymerization of the cationic monomer. After cooling to room temperature, the reaction mixtures became very turbid upon increasing the DP. The VB-270 reaction mixture even turned to a very viscous gel-like solution. The conversions of the reactions were obtained from the NMR spectra by calculating the changes in the integrals of the aromatic and double bond signals. The degree of polymerization of VBTMA in the block copolymers were determined by taking the PEG signal as a reference. The ratios between the two blocks were also determined from the PEG repeating units. The structure of the block copolymers VB-*n* is shown in Scheme 1.

Scheme 1. Block Copolymer VB-*n* with Triflate Counterion
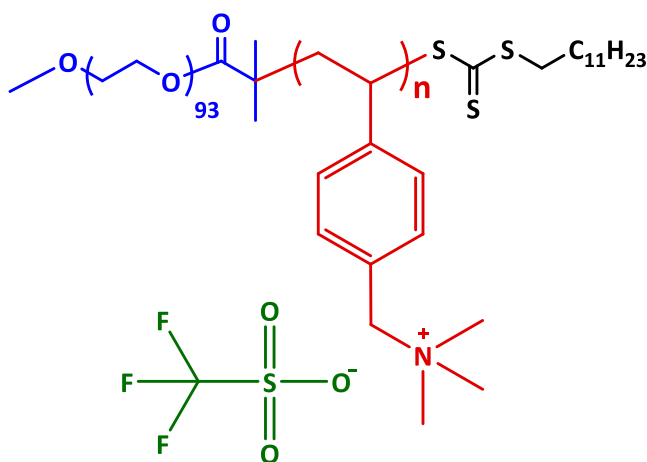
The end group, dodecyl trithioester, of the VB-62 was removed by reacting with an excess of AIBN (Scheme S2). UV−vis spectroscopy confirmed the successful removal of the end group in VB-62, and the absorbance from trithioester totally disappeared; see the Supporting Information, Figure S2.

Molecular Mass Effect on Phase Separation. The solution properties of block copolymers were investigated in aqueous triflate solutions as a function of temperature and LiOTf concentration. All block copolymers are soluble in pure water, but they phase separate in the presence of LiOTf. It is worth noting this is not an ordinary salting-out phenomenon. No phase separation was observed in 50 mM aqueous NaCl solution of VB-172, and in addition, we have previously studied saline solutions of VB-81, which do not phase separate either.[17] The first observations were made by measuring the transmittances of the solutions. Most of the measurements were conducted by keeping the polymer concentration constant and changing the LiOTf concentration. The cloud

point temperature T_{cU} and clearing temperature T_{cL} were taken from the transmittance curves as shown in Figure S3.

Transmittance of the Solutions of the Shortest Diblock Copolymer, VB-62. The solutions of VB-62 were transparent at all temperatures in pure water and in low LiOTf concentrations. However, the cloudiness appeared with increasing salt, from 30 mM up to 1 M. A similar stepwise phase separation was observed in aqueous VB-62 triflate solutions as was earlier detected with VB-81.[17] Upon cooling, the clear polymer solutions turned to turbid at T_{cU} and then became clear at T_{cL} with further cooling (Figure 1). The
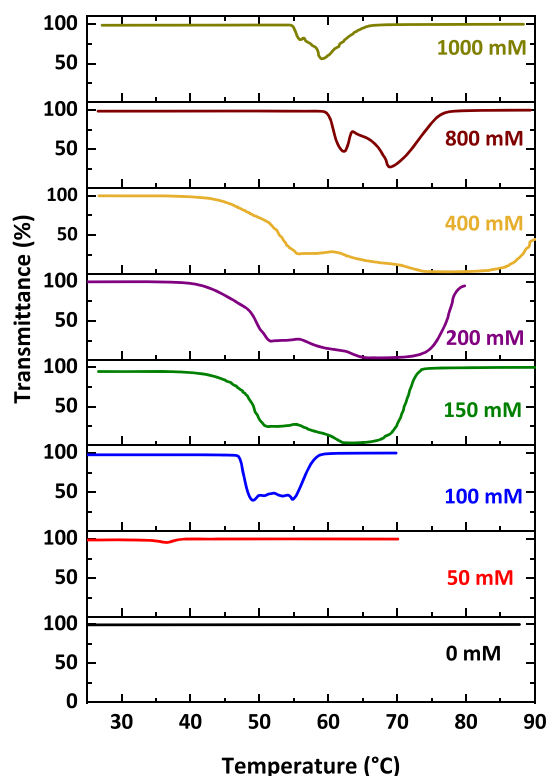

Figure 1. Data collected upon cooling. Transmittance curves for VB-62 solutions with constant polymer concentration (1 mg mL^{-1}) and various LiOTf concentrations. The lowest salt concentration showing any turbidity is 50 mM.

transmittance curves show several minima because of the interplay of various interactions. However, changing the cooling rate within the range 0.1−10 °C min^{-1} does not essentially change the shape of the curves; see Figure S5. The cloud points T_{cU} and the clearing points T_{cL} for VB-62 with constant polymer concentration (1 mg mL^{-1}) are shown in Figure 2. Significant changes were observed in the phase separation of VB-62 with increasing the salt concentration. With salt concentration 150 mM and higher, clearing of the solution occurred stepwise upon cooling. A similar trend was also observed in the heating cycle (Figure S4); the solution clouded stepwise at T_{cL} upon heating and cleared again at high temperatures (T_{cU}).

The short polymer VB-62 differs from the one we studied earlier, VB-81. First, the shorter polymer has much wider insolubility window and second, the transmittance of VB-62 almost reaches 100% at lowest temperatures. VB-81 solutions were always turbid at room temperature. At high salt concentrations one can observe both phase separation and
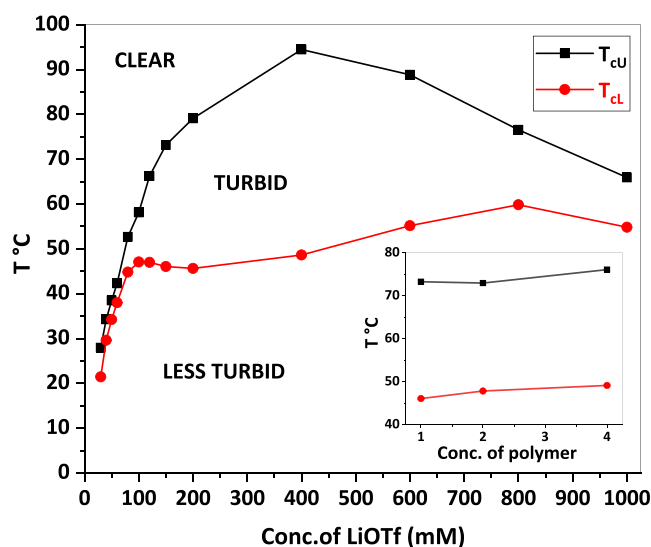
Figure 2. T_{cL} and T_{cU} points for VB-62 in various LiOTf concentration upon cooling. At temperatures below T_{cL} the transmittance never reaches 100%, and the solution is "less turbid". In the inset, the T_{cL} and T_{cU} for the VB-62 with different polymer concentration in constant 150 mM LiOTf solutions.

Figure 3. Transmittance curves for (A) copolymer VB-172; (B) copolymer VB-270 in LiOTf solutions with constant polymer concentration (1 mg mL^{-1}). Heating and cooling rates in A and B are 1° min^{-1}. (C) Cloud point temperatures (T_{cU}) for both polymers. (D) Transmittance curves for VB-172 (1 mg mL^{-1}) in 50 mM LiOTf with different cooling rates. ∗ in part A indicates the very weak clearing step; see the text.

remixing for VB-62 whereas VB-81 only undergoes an UCST type phase separation.[17] In the phase diagram in Figure 2, T_{cU} and T_{cL} follow the same trend up to the salt concentration 150 mM, but diverge with further increasing the salt. The T_{cU} decreased with increasing the LiOTf from 400 to 1000 mM. A similar trend was observed earlier in the case of poly(2-methacryloyloxyethyltrimethylammonium iodide) (PMOTAI) homopolymer solution in the presence of LiOTf and KOTf.[5]

Finally, we needed to test the effect of the polymer concentration on the phase behavior, and for the experiments, we used VB-62. The transmittance curves collected for VB-62 with different polymer concentrations in 150 mM LiOTf are shown in Supporting Information, Figure S5. The T_{cU} of the VB-62 shifted to higher temperature with increasing the polymer concentration as the number of cationic units increased. The clearing temperature T_{cL} did not change considerably, compared to VB-81, but the transmittance of the solutions at low temperature decreased.

Copolymers VB-172 and VB-270. The molar masses of the polymers VB-172 and VB-270 are high, and the differences in their behavior are minor. The solutions were clear in water but became turbid when adding LiOTf. Here, 20 mM LiOTf was required to observe cloudiness. Transmittance curves measured both upon cooling and heating are shown in parts A and B of Figure 3 for both polymers as a function of LiOTf concentration. For high molar mass polymers, only one UCST type change could be observed regardless of the salt concentration. VB-172 in a way resembles the shorter VB-81 (previous report[17]): a very weak clearing step was observed upon heating around 50 °C (see ∗ in Figure 3A). The phase diagrams for VB-172 and VB-270 are almost identical (Figure 3C) and are certainly different from that of VB-62. Only minimal hysteresis was observed for the high molar mass polymers upon cooling and heating scans, thus indicating the dynamic nature of the colloid particles. The big polymers are sensitive to the cooling rate, see VB-172 as an example in Figure 3D. Upon fast cooling small particles build up and
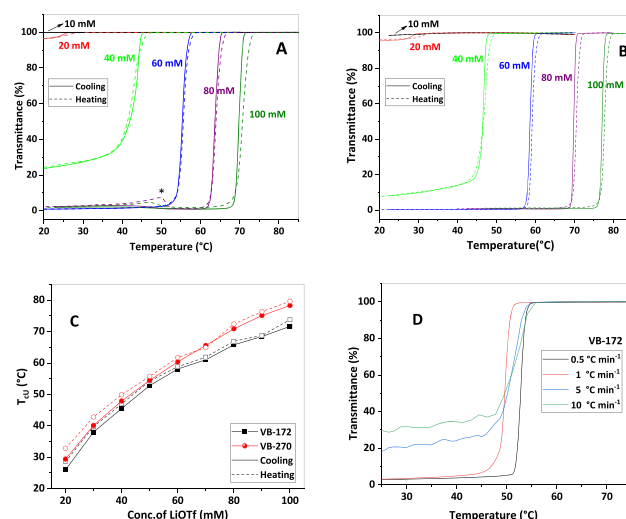
transmittance does not immediately drop to zero. The time dependence of the further aggregation was not studied.

Summary of the Molecular Weight Effect. Removal of the End Group. The length of the polycation block turned out to have a critical effect on the thermal behavior of the polymers. This is well illustrated in Figure 4. The measured transmittance curves of the block copolymer solutions in a constant 50 mM LiOTf concentration showed that the chains with longest cationic blocks phase-separated in a UCST transition. In the short polymers, the phase separation took place in a stepwise manner and was followed by at least partial remixing. The shorter was the cationic block, the higher was the PEG:cation ratio and more steadily the polymers redissolved at low temperature. The transmittance at room temperature is almost 100% in the case of VB-62. We have earlier concluded that the phase separation of VB-81 is strongly dependent on the salt concentration. This is correct but we see now that the ratio of the block lengths is equally essential.

A hydrophobic chain in the end of a polymer turns it semitelechelic, which may affect the micellization behavior. To see the effect explicitly in the present case, the alkyl chain was removed from VB-62 with extra amount of AIBN; this led to the polymer VB-62-EM. The transmittance measurements for VB-62-EM were conducted in LiOTf solutions with different salt concentrations. The transmittance curves measured upon cooling for VB-62-EM in 100 and 200 mM LiOTf are shown in Figure 4 (right). Removing the hydrophobic unit shifted T_{cU} and T_{cL} to lower temperatures in all solutions, the change being 1−2 °C. However, the phase demixing/remixing process of VB-62 did not change.

Light Scattering Studies on Diblock Copolymer Solutions. Electrophoretic Mobilities. The transmittance data were complemented by measuring the size distributions of the colloid particles by light scattering. The measurements were conducted using back scattering at 173° angle as a function of temperature. First, the solutions were stabilized at elevated temperature, and then the scattered intensities and
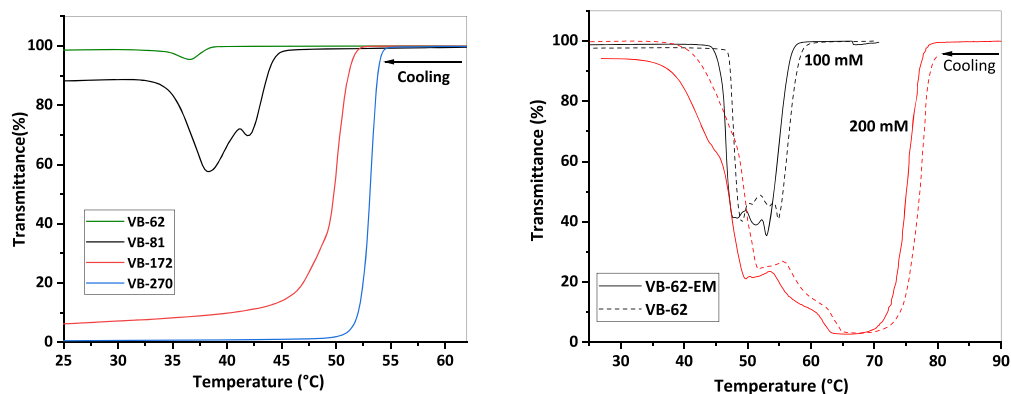
Figure 4. Transmittance curves upon cooling, (left) copolymers VB-62, VB-81(∗), VB-172, and VB-270 in 50 mM LiOTf solutions with constant polymer concentration (1 mg mL^{-1}); Transmittance curves for VB-62 and end modified VB-62-EM polymers in 100 and 200 mM LiOTf salt solutions (right). (∗) Data from ref 17.
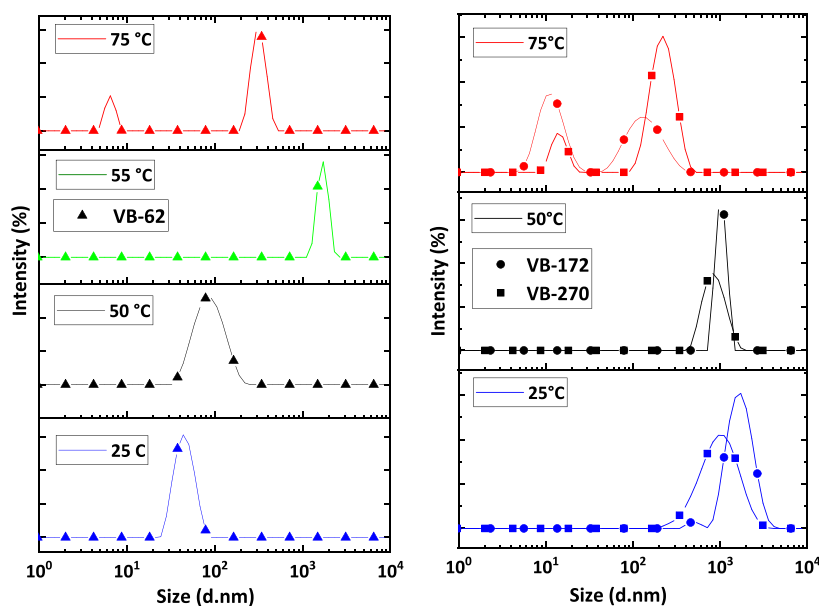

Figure 5. Size distributions measured at 173° scattering angle for VB-62 (▲) in 150 mM (left) and VB-172 (●) and VB-270 (■) (right) in 50 mM LiOTf solutions, polymer concentration 2 mg mL^{-1}.

average size distributions were collected upon stepwise cooling with 5 °C intervals. Temperature-dependent intensity-averaged size distributions are plotted in Figure 5, for VB-62 on the left and for the high molar mass polymers on the right side. Different salt concentrations were used in different cases. For VB-62 this was 150 mM and for VB-172 and VB-270 mM. In 50 mM salt solution the insolubility window for VB-62 is very narrow, and it was found to be sensible to widen it with extra salt. The size distributions for VB-62 in 50 mM are, however, reported in the Supporting Information (Figure S6). Size distributions in Figure S6 are closely similar to those published earlier for VB-81in similar salt concentration.[17]

At 75 °C, all polymer solutions showed bimodal size distribution with small sizes below 10 nm, which indicates the polymers were dissolved on the molecular level. The peak positioned at over 100 nm originates from the polyelectrolyte effect; i.e., it is a result of the "slow mode" often observed in polyelectrolyte solutions with low or moderate ionic strengths.[23,24] Note that the polyelectrolyte peak disappears at lower temperatures. This is an important finding giving

information on the structures of the colloid particles. As the solution of VB-62 cooled to 55 °C, the polymer formed very large particles/aggregates, of the order of 1000 nm. However, upon further cooling to 50 °C and below, the large aggregates gradually dispersed in to small ones, with diameters below 100 nm. The angular dependency measurements (data not shown) conducted at 25 °C indicated that the VB-62 has assembled into spheres with loose cationic cores and PEG coronas. The core–shell structure well explains the disappearance of the polyelectrolyte peak. The average size distributions measured for VB-172 and VB-270 in 50 mM LiOTf solutions were mutually very similar (Figure 5, right). Upon cooling both polymers phase-separated into large aggregates at 50 °C. Different from VB-62, the aggregates of the big polymers did not disintegrate upon further cooling to 25 °C. The structures of the colloid particles were frozen, as we shall discuss later.

The scattered light intensity data collected from the solutions at different temperatures followed similar trends with transmittance results. In VB-62 polymer solution (Figure S7), the scattered intensities showed a sudden maximum at 55

Scheme 2. Illustration of the Colloid Particles Formed by the Polymers: (A) VB-62; (B) VB-172; (C) VB-270
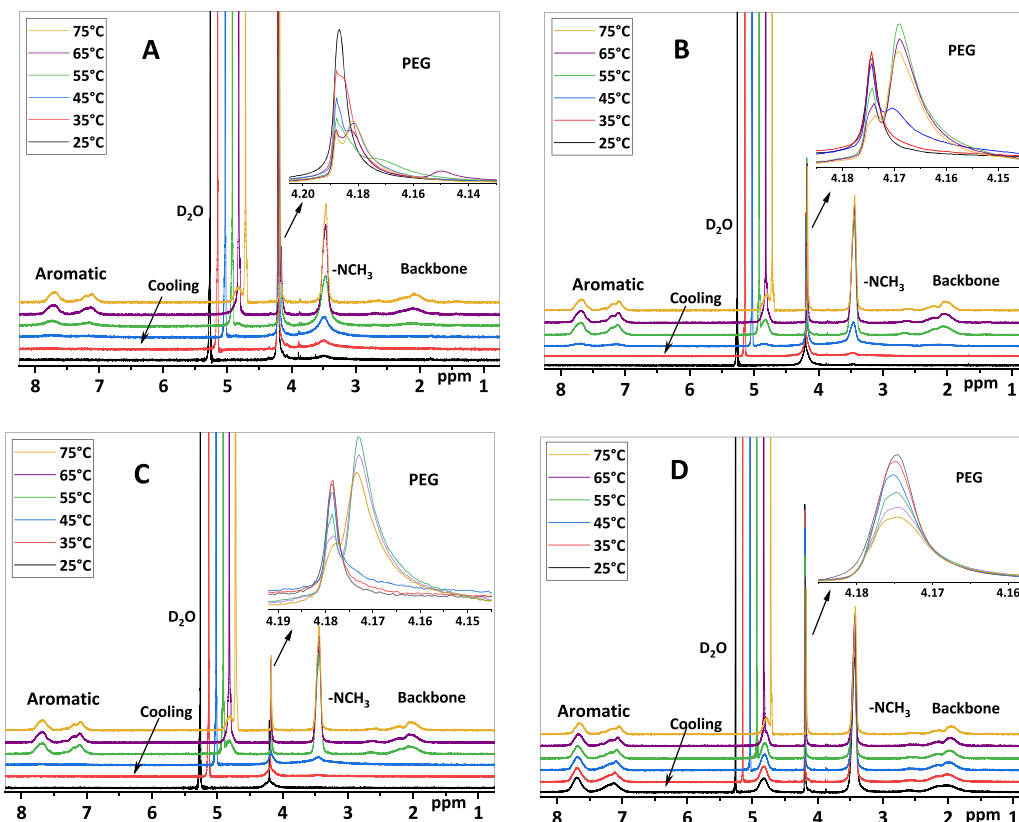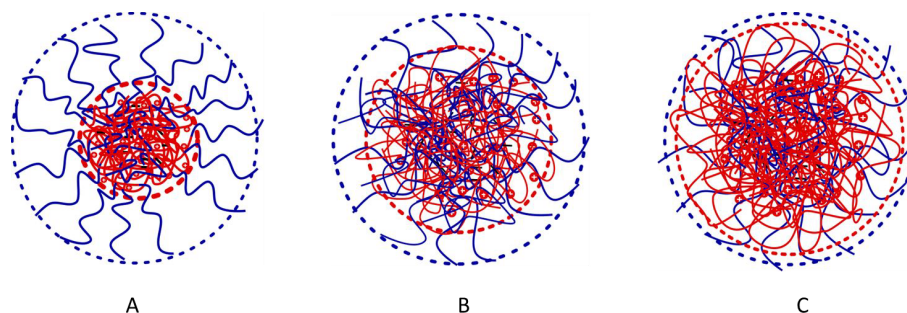

Figure 6. ^{1}H NMR spectra of copolymers collected at various temperatures upon cooling: (A) 2 mg mL^{-1} of VB-62 in 150 mM LiOTf, (B) 2 mg mL^{-1} of VB-172 in 50 mM LiOTf, (C) 2 mg mL^{-1} of VB-270 in 50 mM LiOTf, and (D) 2 mg mL^{-1} of VB-172 in pure deuterated water.

°C, after the phase separation. The scattered light intensities of VB-172 and VB-270 only monotonously increased upon cooling. On the basis of the transmittance and light scattering data, we can draw conclusions on the balance between various interactions in solutions/dispersions with varying temperatures. The changes in this balance critically change the demixing/remixing process. The structures suggested for particles/aggregates for the polymers are shown in Scheme 2. Note that the particles of VB-62 are sterically stabilized by the PEG blocks whereas the particles of VB-270 are electrostatically stabilized by the charges from the polymer and the counterion. VB-172 is between these two extremes. The model helps to understand the processes occurring while temperature decreases. VB-62 formed large aggregates but while the PEG blocks wound to the outer shell the aggregates disperse into smaller, stable particles. On the other hand, VB-270 builds up large hydrophobic particles stabilized with ionic charges.

The electrophoretic mobilities μ measured for the three polymers support the above drawn picture. The mobilities depend strongly on the salt concentration, and we decided to use 50 mM because this is a concentration where differences between the polymers are easily detected (see, e.g., Figure 4). The short polymer VB-62 has μ equal to 0.75 μm cm/(V s) at 65 °C and the corresponding value at 25 °C is 0.094 μm cm/(V s). This means we are observing positively charged entities at both temperatures. Longer polymers VB-172 and VB-270 change their mobility values from positive to negative after cooling, evidently because the collapsed particles are not shielded by PEG chains. Triflate anions are observed to be crowding around the cationic charges of the particle surfaces.

Demixing and Remixing Seen through NMR. The molecular weight dependence and interactions involved in the phase separation process of PEG-polycation were investigated by ^{1}H and NOESY NMR. The ^{1}H NMR spectra collected at
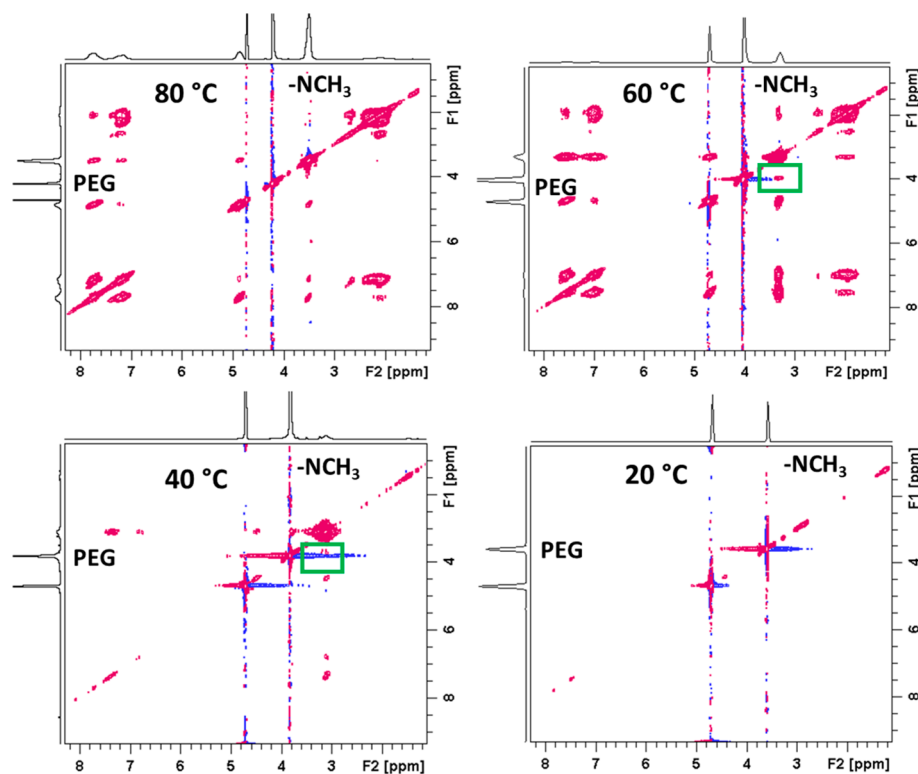
Figure 7. ^1H–^1H NOESY spectra for the VB-62 in D_2O with 150 mM LiOTf at different temperatures. The cross-peaks of PEG and the cation are marked with green boxes.
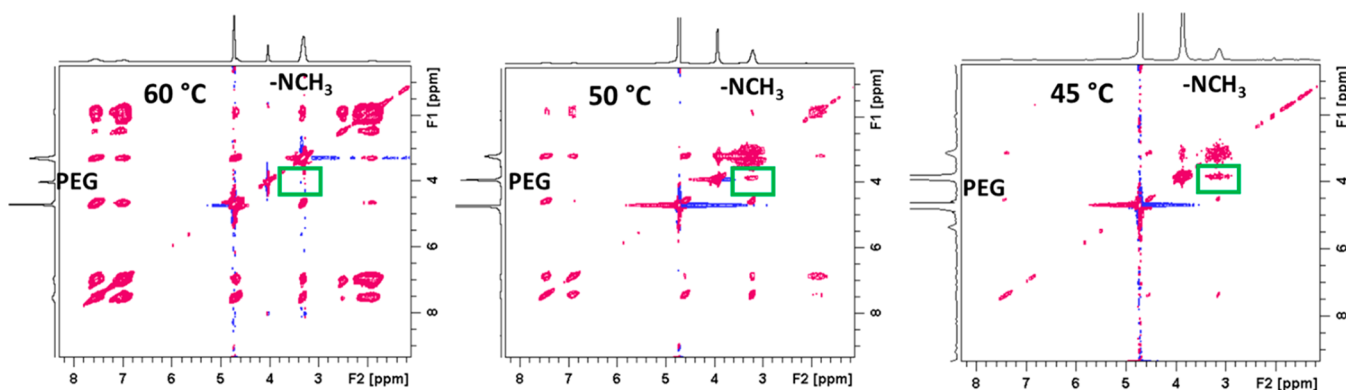

Figure 8. ^1H–^1H NOESY spectra for the VB-270 in D_2O with 50 mM LiOTf.

various temperatures for the different copolymer solutions are presented in Figure 6. In all cases (A−C), the signals arising from the cationic block disappeared upon cooling because of the phase separation. The spectra indicate the polycation block got immobilized in the core of colloid particles and was covered by a PEG corona. In the case of VB-172 in pure D_2O (Figure 6D) there were no changes in the peaks of the polycation because the phase separation of the PEG-polycation is only observed in the presence of LiOTf. However, the PEG signal changed. The PEG signal height increased with decreasing temperature though almost no changes were observed in the integrated intensities.

The temperature dependence of the PEG signal was remarkable in the presence of added LiOTf or NaCl; see Figure 6 and Supporting Information, Figure S8B. The PEG signal split into two (or even three in VB-62) at elevated temperatures. This splitting was not observed in pure D_2O.

Note also, that the plain PEG macromonomer dissolved in aqueous LiOTf gave only a singlet peak, the intensity of which decreased with increasing temperature, Figure S8A. The integrated intensity kept practically constant. In addition, with increasing LiOTf concentration (Figure S8C), the PEG signal of VB-172 showed three peaks at 65 °C, just below the cloud point temperature. The findings indicate that the interactions between the two blocks existed even at high temperatures and they are mediated by the triflate anions. Comparison of the PEG signals at 75 °C shows that the upfield component increases in strength when the DP of the polycation increases and thus, the highfield line arises from the PEG bound to the polycation.

At low temperature, only one line was observed for PEG; however, it probably was a superposition of a broad and a narrow spectral lines. The height of the signal changed depending on the DP of the polycation, decreasing with

increasing length of the polycation. In VB-270, the PEG signal was least intense and clearly broadened, thus indicating that most of the polyether was buried in the core of the particle and only few free chains were dangling on the surface.

2D $^1H-^1H$ NOESY spectroscopy gives information on the through space interactions in polymer systems. The spectra collected at different temperatures for the VB-62 in D_2O with 150 mM LiOTf are shown in Figure 7 and those for VB-270 in 50 mM LiOTf in Figure 8. Weak cross-peaks between the PEG and $-NCH_3$ protons were observed within the temperature range from 70 to 40 °C. In the case of VB-172 in 50 mM LiOTf (not shown) solutions, the cross-peaks from the interaction of PEG and NCH_3 were only observed at 45 °C where the polycation phase-separated. This is a molecular level indication of the interaction between the blocks and shows that within the insolubility window (VB-62) or at temperatures below T_{cU} (VB-172 and 270) the protons of different blocks are at very close proximity.

CONCLUSIONS

Mechanisms of demixing and remixing of PEG–polycation block copolymers have been studied using polymers with varying lengths of the cationic block. The polymers were synthesized via RAFT polymerization in aqueous methanol mixtures using a PEG-based chain transfer agent. The block ratios of the polymers were changed with targeting different degrees of polymerization of the cationic monomer, vinylbenzyl trimethylammonium triflate, VBTMA. The polymers were named with acronyms VB-n, where n is the DP of the cationic block. The molar mass of PEG was 5000. We used as a reference VB-81, which has been studied previously.[17] From one of the polymers, the trithioester end group was removed through a reaction with AIBN. The phase separation processes were investigated in aqueous triflate (LiOTf) solutions. The polymer with the shortest VBTMA block phase-separated upon cooling but almost totally mixed again when temperature was further decreased, whereas the polymers with high VBTMA content phase-separated in a single step. Transmittance and DLS measurements showed the temperature of phase separation, as well as the width of the insolubility window in the case of the short polymers depend on the block ratio and LiOTf concentration. The end groups, dodecyl chains did not affect the main phase separation process though the transition temperatures slightly shifted.

The polymers VB-62 and VB-81 turn cloudy at T_{cU} upon cooling and partially clear at even lower temperature, T_{cL}. Polymers VB-172 and VB-270 phase separate in one step upon cooling. These processes were studied with NMR in D_2O/OTf solutions. In ^1H NMR spectra, the signals from the cationic blocks disappeared with decreasing temperature because of the phase separation. The PEG signals from the block copolymers split into two. Of the two lines, the one at higher field was concluded to originate from the PEG units in close interaction with cationic units of the polymer and it increased in strength when the samples were cooled. NOESY measurements showed that in the shortest polymer, VB-62, at least part of the protons of PEG and the methyl groups in the polycation are in a very close proximity within the insolubility window. In a longer chains, VB-172 and VB-270, cross-correlation peaks were observed at very beginning of the phase separation.

To sum up, we have shown that the polymers assemble into big particles/aggregates when hot transparent solutions are cooled. Upon further cooling, VB-62 particles disperse into smaller ones; this was not observed for VB-172 or VB-270 particles. On the basis of the findings, we suggest that VB-62 colloid particles are at low temperatures sterically stabilized with PEG chains, whereas in the dispersions of VB-270 the PEG chains are buried inside the cationic core and the particles are stabilized by the surface charges. VB-172 dispersions show features of both bigger and smaller polymers.

ASSOCIATED CONTENT

Ⓢ Supporting Information

The Supporting Information is available free of charge on the ACS Publications website at DOI: 10.1021/acs.macro-mol.9b01327.

> End group modification and UV–vis spectrum of VB-62, ^1H NMR spectrum of VB-n, transmittance curves for VB-62, light scattering data, and temperature variant ^1H NMR spectra (PDF)

AUTHOR INFORMATION

Corresponding Author

*(H.T.) E-mail heikki.tenhu@helsinki.fi.

ORCID Ⓞ

Vikram Baddam: 0000-0001-5327-9066
Sami Hietala: 0000-0003-1448-1813
Heikki Tenhu: 0000-0001-5957-4541

Notes

The authors declare no competing financial interest.

ACKNOWLEDGMENTS

REFERENCES

(1) Vijayakrishna, K.; Mecerreyes, D.; Gnanou, Y.; Taton, D. Polymeric Vesicles and Micelles Obtained by Self-Assembly of Ionic Liquid-Based Block Copolymers Triggered by Anion or Solvent Exchange. *Macromolecules* 2009, 42 (14), 5167–5174.

(2) Vijayakrishna, K.; Jewrajka, S. K.; Ruiz, A.; Marcilla, R.; Pomposo, J. A.; Mecerreyes, D.; Taton, D.; Gnanou, Y. Synthesis by RAFT and Ionic Responsiveness of Double Hydrophilic Block Copolymers Based on Ionic Liquid Monomer Units. *Macromolecules* 2008, 41 (17), 6299–6308.

(3) Guo, J.; Zhou, Y.; Qiu, L.; Yuan, C.; Yan, F. Self-Assembly of Amphiphilic Random Co-Poly(Ionic Liquid)s: The Effect of Anions, Molecular Weight, and Molecular Weight Distribution. *Polym. Chem.* 2013, 4 (14), 4004.

(4) Yoshimitsu, H.; Kanazawa, A.; Kanaoka, S.; Aoshima, S. Well-Defined Polymeric Ionic Liquids with an Upper Critical Solution Temperature in Water. *Macromolecules* 2012, 45 (23), 9427–9434.

(5) Karjalainen, E.; Aseyev, V.; Tenhu, H. Counterion-Induced UCST for Polycations. *Macromolecules* 2014, 47 (21), 7581–7587.

(6) Niskanen, J.; Tenhu, H. How to Manipulate the Upper Critical Solution Temperature (UCST)? *Polym. Chem.* 2017, 8 (1), 220–232.

(7) Biswas, Y.; Maji, T.; Dule, M.; Mandal, T. K. Tunable Doubly Responsive UCST-Type Phosphonium Poly(Ionic Liquid): A Thermosensitive Dispersant for Carbon Nanotubes. *Polym. Chem.* 2016, 7 (4), 867–877.

(8) Liu, C.; Wang, S.; Zhou, H.; Gao, C.; Zhang, W. Thermoresponsive Poly(Ionic Liquid): Controllable RAFT Synthesis, Thermoresponse, and Application in Dispersion RAFT Polymerization. *J. Polym. Sci., Part A: Polym. Chem.* 2016, 54 (7), 945–954.

(9) Kohno, Y.; Deguchi, Y.; Inoue, N.; Ohno, H. Temperature-Driven and Reversible Assembly of Homopolyelectrolytes Derived

from Suitably Designed Ionic Liquids in Water. *Aust. J. Chem.* **2013**, *66* (11), 1393.

(10) Karjalainen, E.; Aseyev, V.; Tenhu, H. Upper or Lower Critical Solution Temperature, or Both? Studies on Cationic Copolymers of N-Isopropylacrylamide. *Polym. Chem.* **2015**, *6* (16), 3074−3082.

(11) Tauer, K.; Weber, N.; Texter, J. Core-Shell Particle Interconversion with Di-Stimuli-Responsive Diblock Copolymers. *Chem. Commun.* **2009**, No. 40, 6065−6067.

(12) Mori, H.; Yahagi, M.; Endo, T. RAFT Polymerization of N-Vinylimidazolium Salts and Synthesis of Thermoresponsive Ionic Liquid Block Copolymers. *Macromolecules* **2009**, *42* (21), 8082−8092.

(13) Men, Y.; Drechsler, M.; Yuan, J. Double-Stimuli-Responsive Spherical Polymer Brushes with a Poly(Ionic Liquid) Core and a Thermoresponsive Shell. *Macromol. Rapid Commun.* **2013**, *34* (21), 1721−1727.

(14) Longenecker, R.; Mu, T.; Hanna, M.; Burke, N. A. D.; Stöver, H. D. H. Thermally Responsive 2-Hydroxyethyl Methacrylate Polymers: Soluble-Insoluble and Soluble-Insoluble-Soluble Transitions. *Macromolecules* **2011**, *44* (22), 8962−8971.

(15) Zhang, Y.; Tang, H.; Wu, P. Multiple Interaction Regulated Phase Transition Behavior of Thermo-Responsive Copolymers Containing Cationic Poly(Ionic Liquid)S. *Phys. Chem. Chem. Phys.* **2017**, *19* (45), 30804−30813.

(16) Han, X.; Zhang, X.; Yin, Q.; Hu, J.; Liu, H.; Hu, Y. Thermoresponsive Diblock Copolymer with Tunable Soluble-Insoluble and Soluble-Insoluble-Soluble Transitions. *Macromol. Rapid Commun.* **2013**, *34* (7), 574−580.

(17) Baddam, V.; Aseyev, V.; Hietala, S.; Karjalainen, E.; Tenhu, H. Polycation-PEG Block Copolymer Undergoes Stepwise Phase Separation in Aqueous Triflate Solution. *Macromolecules* **2018**, *51* (23), 9681−9691.

(18) Jana, S.; Biswas, Y.; Anas, M.; Saha, A.; Mandal, T. K. Poly[Oligo(2-Ethyl-2-Oxazoline)Acrylate]-Based Poly(Ionic Liquid) Random Copolymers with Coexistent and Tunable Lower Critical Solution Temperature- and Upper Critical Solution Temperature-Type Phase Transitions. *Langmuir* **2018**, *34* (42), 12653−12663.

(19) Zheng, Z.; Zhang, L.; Ling, Y.; Tang, H. Triblock Copolymers Containing UCST Polypeptide and Poly(Propylene Glycol): Synthesis, Thermoresponsive Properties, and Modification of PVA Hydrogel. *Eur. Polym. J.* **2019**, *115*, 244−250.

(20) Ge, C.; Liu, S.; Liang, C.; Ling, Y.; Tang, H. Synthesis and UCST-Type Phase Behavior of α-Helical Polypeptides with Y-Shaped and Imidazolium Pendants. *Polym. Chem.* **2016**, *7* (38), 5978−5987.

(21) Li, M.; He, X.; Ling, Y.; Tang, H. Dual Thermoresponsive Homopolypeptide with LCST-Type Linkages and UCST-Type Pendants: Synthesis, Characterization, and Thermoresponsive Properties. *Polymer* **2017**, *132*, 264−272.

(22) Zhao, L.; Zhang, L.; Zheng, Z.; Ling, Y.; Tang, H. Synthesis and Properties of UCST-Type Thermo- and Light-Responsive Homopolypeptides with Azobenzene Spacers and Imidazolium Pendants. *Macromol. Chem. Phys.* **2019**, *220*, 1900061.

(23) Mandel, M. In *Dynamic Light Scattering: The Method and Some Applications*; Brown, W., Ed.; Clarendon Press: Oxford, U.K., 1993; Chapter 7, p 319.

(24) Muthukumar, M. 50th Anniversary Perspective: A Perspective on Polyelectrolyte Solutions. *Macromolecules* **2017**, *50* (24), 9528−9560.